Journal of Nonlinear and Convex Analysis
Volume 26, Number 6, 2025, 1823–1840

Yokohama Publishers
ISSN 1880-5221 ONLINE JOURNAL

REAL-TIME ALIGNMENT COMPENSATION PREDICTION FOR FLEXIBLE FILM EXPOSURE MACHINE BASED ON GENETIC ALGORITHM OPTIMIZING BACK-PROPAGATION NEURAL NETWORK

JIANPU XI*, ZIKAI NIE, LIJUAN DENG, YONGGAO YUE, AND QING YANG

Abstract. A genetic algorithm-optimized backpropagation (BP) neural network is utilized to forecast real-time alignment correction for a flexible-film exposure machine. In this study, the compensation value of a compensation system used in the alignment of an exposure machine is predicted using an optimal neural network. Subsequently, the anticipated value is juxtaposed with the factual compensation value, and its compliance with alignment standards is evaluated. A compensation design of an exposure machine is verified experimentally, hence validating the effectiveness of the suggested approach for real-time alignment compensation pre-diction. The suggested method outperforms a single backpropagation neural network model in terms of system sensitivity and resilience, lowering mean square error by 70.99% and exposure-machine alignment time by 27.4%, rendering the improvements beneficial for engineering applications.

1. Introduction

The flexible-film exposure device is typically employed in the exposure phase of printed circuit board (PCB) fabrication. The device is a high-precision instrument used for developing complex circuits and patterns on dielectric film substrates. It uses a light source to transmit through a photomask and transmit predefined patterns or circuits onto the surface of a thin film by light radiation. The resulting designs are widely used in the production of flexible electronic appliances such as smartphone screens, tablets, flexible displays, and sensors. The revival of the global economy and Industry 4.0 efforts, such as China Smart fabrication 2025, have created technological problems in the production precision and efficiency of flexible-film exposure machines, which are essential components in the production of circuit boards. As a result, improving their current accuracy and efficiency has drawn attention. An effective alignment compensation prediction can minimize the number of alignment process repeats while simultaneously increasing alignment precision, optimizing the exposure impact, and improving compensation selection accuracy.

2020 *Mathematics Subject Classification.* 93B35, 93B45, 93B47.

Key words and phrases. Exposure machine, alignment compensation prediction, genetic algorithm, backpropagation neural network, compensation design.

National Natural Science Foundation of China funded project (51705546), Natural Science Foundation of Henan Province (242300421259), Zhongyuan University of Technology Nature Fund Project (K2023MS015), Key Laboratory of Optical Sensing and Testing Technology in Mechanical Industry (2022SA-04-15), Guiding project of China National Textile and Apparel Council(2020073).

*Corresponding author.

The current alignment compensation procedures are divided into three categories: Taguchi methods, single-factor methods, and methods based on artificial intelligence and machine learning. In addition to being time-consuming and difficult to utilize, Taguchi methods rarely deliver desired alignment effects and thus demand for a high degree of knowledge and significant experience. In a similar vein, single-factor approaches remain short of accomplishing the intended alignment effects even if they show faster selection rates than Taguchi methods yield. The subsequent compensation impact is directly determined by the elements that influence the alignment effect while selecting compensation value [11]. To accomplish a specific degree of compensation effect utilizing these approaches, a great deal of expertise and experience are required because to the nonlinearity and uncertainty inherent in the exposure-machine alignment correction system.

The application of machine learning techniques can effectively address the prediction problem in large-scale data, enhance real-time data processing capabilities, and expedite the process of identifying the optimal data solution, thereby improving the expected compensation effect [12]. It can also vividly depict the relationship between data and the alignment compensation system. For example, Tsai et al [18] introduced a data-driven approach for modelling the system integration scale factor and positioning performance of an exposure machine. Their model not only predicts positioning errors but also analyses parameter sensitivity. Similarly, Chou et al [2] optimized the parameter combinations of multilayer convolutional neural networks using a unified experimental design, thereby improving network performance and enhancing image recognition accuracy for exposure machines through integrated factorial experiments. Ahmadi et al [1] developed a method based on genetic algorithms to swiftly compute the center of a circle in automatic exposure machine image localization and applied it to a 4CCD automatic monitoring and exposure machine.

In order to improve the automated alignment speed of an exposure machine, Malashkhia et al. [15] integrated reference coordinates with intelligent image recognition. This method achieved positional precision of 1 to 4 μm along the X and Y-axes, with an auto-alignment time of around 10 s. An image alignment method was developed by Malashkhia et al. [15] that improves imagine matching and alignment efficiency by using pattern matching to ex-tract features from target information. Meanwhile, Ghiasian et al. [4] developed a two-step auto-alignment system that relies on geometric correlations between measurement data and machine coordinates. This algorithm deter-mines the compensation value by reducing the positioning error. The study on alignment markers by Kwon and Hwang showed that geometric template matching can improve the speed of recognition, surpassing traditional correlation-based matching [9]. This suggests that artificial intelligence and machine learning can significantly enhance image recognition accuracy and precision, speed up alignment, and reduce compensation value errors in exposure machine alignment compensation.

The objective of this study was to investigate the real-time prediction of alignment compensation for an expo-sure machine. In addition to offering a suitable compensation parameter design that adapts appropriately to overall platform changes during the exposure machine's alignment process and enhances alignment accuracy,

this configuration uses a uniform design to enable the experimental methods to process the compensation value data. The effect of the compensation value was then evaluated using a backpropagation (BP) neural network that was genetic algorithm-optimized. This facilitated the prediction of alignment results for the flexible-film exposure machine. The prediction efficiency and accuracy provided by the single BP neural network and the BP neural network improved by the genetic algorithm are compared in the experimental results [8,10]. The results show that the proposed re-al-time alignment compensation system reduces repetitions, increases production efficiency, and significantly improves alignment precision.

2. Alignment compensation parameter design

Research studies have focused on improving the precision and efficiency of the alignment step in exposure machines used in PCB manufacturing, especially in the face of miniaturization and increased complexity. The standard alignment method of an exposure machine depends primarily on manual modifications based on human visual identification, resulting in time-consuming operations and low precision. A high-precision exposure ma-chine's alignment compensation system necessitates the combination of computer vision, motion servo control, multi-coordinate system conversion, vast experimental data, and suitable compensation value formulae [7].

The system, which corrects errors between servo and computer-vision systems, considers factors like vision lens aberration, mechanism design, and assembly accuracy, ensuring alignment and enhancing the productivity of the exposure machine by compensating for anticipated compensation value. Figure 1 illustrates the point alignment process in production, displaying the simulated effect of the alignment compensation system. Figure 2 shows the hardware structure used, while Figure 3 shows the overall alignment lay-out of the exposure machine.

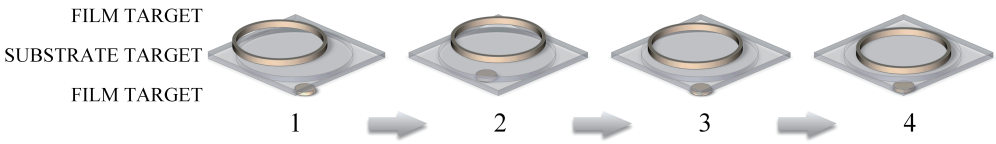

Figure 1. Simulation of alignment error compensation.

An exposure machine's alignment compensation mechanism necessitates the use of two sets of system coordinates to align and expose the objective. This study uses a BP neural network tuned using a genetic algorithm to estimate the compensation value and improve the production accuracy and alignment efficiency of the exposure machine. For the subsequent calculations, it is assumed that (O,X,Y) denotes the coordinate system of the platform where the alignment target is situated; (O_i,X_i,Y_i) denotes the coordinate system of the charge-coupled device (CCD) lens on the exposed object; (XC_i, YC_i) signifies the coordinates of CCD i within the alignment platform coordinates (XC_i, YC_i); and Ti indicates the angle of CCD i within the alignment platform (XC_i, YC_i). The coordinate transformation formula for the CCD coordinate system of the machine and target can be derived by defining the coordinate systems of the alignment target and exposed object, as follows:

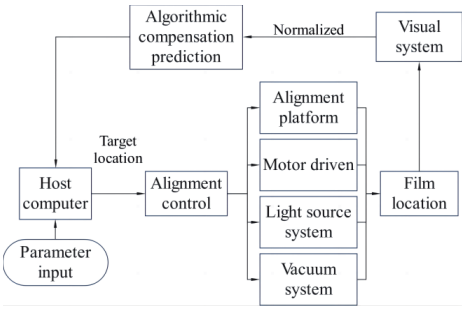

FIGURE 2. Hardware architecture diagram of flexible-film exposure machine for accurate positioning.

$$XT = XC_i + XT_i \cdot \mathrm{COS}(T_i) - YT_i \cdot \mathrm{SIN}(T_i), \tag{2.1}$$

$$YT = XC_i + XT_i \cdot \mathrm{SIN}(T_i) + YT_i \cdot \mathrm{COS}(T_i). \tag{2.2}$$

The alignment errors between the four targets and the upper and lower light masks are denoted by dx_{is}, dx_{ix}, dy_{is}, and dy_{ix}, respectively, whereas $\mathrm{d}D$ is defined as the distance between the alignment centers:

$$dD = \sqrt{dx_i^2 + dy_i^2}. \tag{2.3}$$

Along the X-axis, the difference between the alignment centers of the upper and lower photomasks is expressed by following equation:

$$dX_i = (dx_{1s} + dx_{2s} + dx_{3s} + dx_{4s})/4. \tag{2.4}$$

The difference between the alignment centers of the upper and lower photomasks along the Y-axis is given by:

$$dY_i = (dy_{1s} + dy_{2s} + dy_{3s} + dy_{4s})/4. \tag{2.5}$$

Where $\mathrm{d}T$ is the angular deviation between the upper and lower masks with the template and is given by the following formula:

$$dT = \tan^{-1}\left(\frac{dY}{dX}\right). \tag{2.6}$$

Under the aforementioned conditions, it is evident that when $\mathrm{d}X{=}\mathrm{d}Y{=}0$ and $\mathrm{d}T{=}0$, the exposure machine reaches an optimal alignment state, with the deviation between the vision and servo systems approaching infinitesimal levels, thus leading to the highest quality of exposure [5,20]. The main objective of this research is to achieve rapid convergence of $\mathrm{d}X$, $\mathrm{d}Y$, and $\mathrm{d}T$ to the ideal solution within a limited number of iterations, therefore mitigating the influence of lens aberration, equipment processing accuracy, and platform assembly precision. This turns the exposure machine's alignment compensation prediction into an optimization problem for the three previously indicated parameters. Figure 4 depicts the alignment compensation principle.

The deviations in $\mathrm{d}X$, $\mathrm{d}Y$, and $\mathrm{d}T$ are compensated for by the parameters *fx*, *fy*, and *ft*, respectively. The alignment platform receives continual feedback from

the compensation value, which directs the servomotor to modify the position until alignment is attained. The input parameters *fx*, *fy*, and *ft* of exposure machine are selected, and the X and Y-direction adjustment value, and rotation angle of the alignment platform are compensated to minimize alignment error. To further improve positioning accuracy, we set the following: first-position error: target dX and dY distance difference before pose adjustment (E_1), angle error between initial and first-position points (θ_1), sec-ond-position error: target dX and dY distance difference after pose adjustment (E_2), and angle error between first and second-position points (θ_2). According to the weighted sum of ($|E_1| - |E_2|$) and ($|\theta_1| - |\theta_2|$), when the output result approaches 0, the exposure-machine alignment-compensation prediction system reaches the optimal compensation state, the compensation accuracy of the exposure machine alignment error reaches the ideal state.

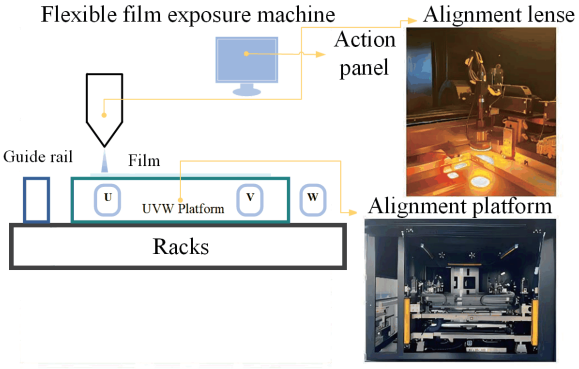

FIGURE 3. Alignment mechanism of flexible-film exposure machine.

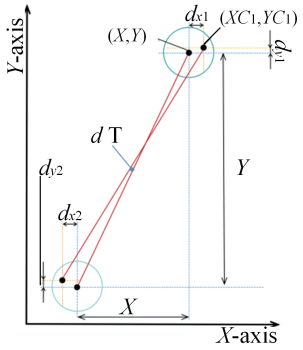

FIGURE 4. Diagram of the principle of alignment compensation.

3. ALIGNMENT ACCURACY ANALYSIS OF FLEXIBLE-FILM EXPOSURE MACHINE

This study employs a BP neural network, augmented by a genetic algorithm, to estimate alignment compensation for an exposure machine and determine the appropriate compensation value to deliver the optimization result. The procedure can be divided into the following three stages: 1) Examine the existing parameter data of the expo-sure machine using a unified experimental design, then process the resulting coordinate data to generate appropriate input and output parameters, evaluate them, and simplify the dataset based on the weight ratio. 2) Train the selected data, refine the model using the BP neural network and genetic algorithm to find the ideal parameters, and then validate accuracy of the model by comparing the training results with the actual parameters. 3) Predict the alignment compensation for the exposure machine employing the evolutionary algorithm-enabled optimized BP neural network, and then compare the results with that of the single BP neural network [3].

3.1. **Compensation parameter acquisition.** The current compensation system parameters, *fx*, *fy*, and *ft*, is required established when a BP neural network optimized by a genetic algorithm is employed for this purpose. The alignment process of an exposure machine requires the collection of advanced and multiple experimental data, which frequently mandates the performance of multifarious experiments that are both complex and time-consuming. When generating data predictions, the compensation system parameters are organized using a consistent experimental design. Simulating each experimental scenario for three parameters is crucial for reducing experiment numbers, uniformly portraying indicator error, enhancing data validity, and ensuring comprehensive comparison, thus enhancing the validity of the data. In subsequent experiments, the comprehensiveness of the data was ensured by identifying 41 experimental conditions based on variations in *fx*, *fy*, and *ft*. The uniform experimental design, which aimed to estimate the alignment compensation for the exposure machine using a non-linear relationship, served as the foundation for the experimental allocation approach. Subsequently, the information needed in accordance with the assessment standards was gathered using the specified methodology [17, 19].

3.2. **BP neural network.** The BP neural network is a multilayer feed-forward network trained using an error BP algorithm, consisting of an input, hidden, and output layer, which can effectively approximate any nonlinear relationship with appropriate parameters. The alignment compensation impact of the expected data is evaluated using the lowest mean square error (MSE) between the actual and predicted values as corrected by the exposure-machine alignment system. The BP neural network can improve prediction results with an appropriate learning function and iterative optimization using the gradient descent principle. However, using the BP neural network for position compensation may not guarantee stability and ineffective optimization due to the need for iterations to approximate optimal neuron weights and thresholds. Implementing this procedure would consume a large number of iterations and negatively affect the accuracy of the results. This study uses a genetic algorithm (GA) to enhance the speed and prediction accuracy of the BP neural network.

3.3. **Genetic algorithm.** Genetic algorithms (GA) emulate the naturally occurring processes of biological evolution. Organisms adapt to changes in their external environment through heredity and mutation. The basic characteristics of the offspring individuals are inherited from the previous generation and differ from those of the previous generation by chance. The strongest adaptive ability individuals are retained during offspring reproduction, resulting in the higher probability of retaining point genes favorable for survival [14, 22]. This algorithm is a parallel, efficient global search method that can automatically search for hidden information in a sample space and iterate to an optimal solution. Numerous studies and experimental results show that while GA offers accuracy in finding optimal values, it also has disadvantages such as slow convergence and a tendency to fall into local optimal solutions.

3.4. **GA optimization of BP neural network.** The process of optimizing a BP neural network using a GA can be divided into three stages:

(1) Determining the structure of the BP neural network;
(2) Optimizing the parameters of the neurons using a GA;
(3) Predicting the alignment compensation for the exposure machine using the optimized BP neural network.

3.4.1. *Determining the structure of the BP neural network.* In this study, a 3-layer BP neural network structure was used. The input parameters are *fx*, *fy*, and *ft*, whereas the output parameters are $(|E_1| - |E_2|)$ and $(|\theta_1| - |\theta_2|)$. The weights and thresholds of each neuron are used to obtain the corresponding output via the activation function, and the error correction of the feedback is obtained. Let each node vector of the input layer be $\mathrm{X} = [x_1, x_2, \ldots, x_i, \ldots, x_l]^T$ for l input neurons. Similarly, let the vector of each node in the hidden layer be $\mathrm{Y} = [y_1, y_2, \ldots, y_i, \ldots, y_m]^T$ for m neurons, and the node vector of the output layer be $\mathrm{Z} = [z_1, z_2, \ldots, z_i, \ldots, z_n]^T$ for n neurons. In addition relationship for different vectors are as follows :

Output vector are

$$\mathrm{D} = [d_1, d_2, \ldots, d_i, \ldots, d_n]^T,$$

Weight vector from the input layer to the hidden layer are

$$\omega = [\omega_1, \omega_2, \ldots, \omega_i, \ldots, \omega_m]^T,$$

Weight vector from the hidden layer to the output layer be

$$\mathrm{E} = [e_1, e_2, \ldots, e_i, \ldots, e_n]^T,$$

Threshold of each node in the hidden layer represented by

$$\theta = [\theta_1, \theta_2, \ldots, \theta_i, \ldots, \theta_m]^T,$$

Threshold of each node in the output layer are

$$\alpha = [\alpha_1, \alpha_2, \ldots, \alpha_i, \ldots, \alpha_n]^T,$$

Weights connecting input layer and hidden layer j be

$$\mathrm{A_j} = \left[A_{j1}, A_{j2}, \ldots, A_{ji}, \ldots, A_{jl}\right]^T,$$

Weights connecting hidden layer and output layer k be

$$\mathrm{B_k} = \left[B_{k1}, B_{k2}, \ldots, B_{ki}, \ldots, B_{kn}\right]^T.$$

The mathematical relationships among the layers are as follows:
For the hidden layer:

$$Y_j = f_{\text{sigmoid}}\left(\sum\nolimits_{a_{jl}} X_l + \theta_j\right). \tag{3.1}$$

For the output layer:

$$Y_k = f_{\text{sigmoid}}\left(\sum\nolimits_{b_{kn}} X_l + \alpha_k\right). \tag{3.2}$$

To avoid the inefficient optimization that occurs when a BP neural network is used to estimate the compensation value for the alignment error of the exposure machine, GA can be used to optimize the weights and thresholds. A GA-optimized

BP (GABP) neural network is a supplemental technique to multi-objective optimization.

3.4.2. *Optimizing the parameters of the neurons using a GA.* The use of a GA in BP neural network initial weights and thresholds accelerates convergence in future training and prevents local optimization issues. The selection of these weights and thresholds depends on the prediction deviation value, which indicates a fitness value. A higher degree of difference results in a smaller fitness value. The selection of a suitable population size is crucial for ensuring spatial sample diversity and prediction accuracy, while minimizing computation time. The number of neurons in the implicit layer depends on the experimental specific data circumstances, determining the optimal number of nodes [6, 16]. The flow of the GA is illustrated in Figure 5.

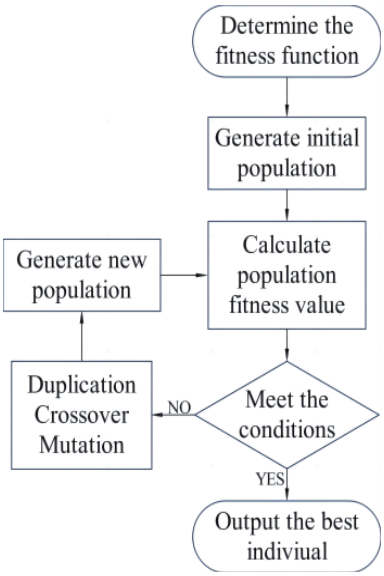

FIGURE 5. Flowchart of GA.

Following assessment of the individual fitness values, individuals are screened for environmental change survival by Selection, Crossover (Pc), and Mutation (Pm) with continuous iterations over the initial population. The selection of genetic operators is crucial to ensuring accuracy. The selection operator selects for individuals with high adaptability to establish an additional generation, with the objective of directly transferring on qualities from out-standing individuals to the next generation. The probability of an individual being selected is given by:

$$P_i = \frac{f_i}{\sum_{k=1}^{n} f^k} = \frac{f_i}{f_{sum}}. \tag{3.3}$$

Where f_i is the fitness value of individual i, and f_{sum} is the fitness value of the population. The crossover operator randomly selects two parent individuals and exchanges their characteristics to generate new individuals. Crossover is of great significance to improving the global optimization ability of the algorithm, and its

fitness is given by:

$$P_c = \frac{f_{\max} - f_i}{f_{\max} - f_{ave}}, f_i \geq f_{ave} \quad P_c = 1.0, f_i < f_{ave} \tag{3.4}$$

where f_{max} is the maximum fitness value, f_{ave} is the average fitness value, and fi is the fitness value of individual i for the crossover. The mutation (Pm) is set independently according to the size of the experimental data and the amount of arithmetic, and the variability of the results is analyzed to ensure that the optimal solution is obtained. Population diversity is a result of selection, crossover, and mutation, respectively. The ideal offspring persons will be utilized as the parents of the following genetic operation's generation once they have been observed through screening. It can be accompanied by an iteration of the selection, crossover, and mutation processes [21]. Until the new generation of weights, the thresholds in the BP neural network for the prediction of the exposure-machine position-error compensation are not in line with the requirements of the pairs. The steps for using the GA to optimize the BP neural network are as follows:

(1) The GA is employed to encode and decode the initial weights and thresholds of the BP neural network, thereby obtaining the initial population. The initial values of the weights and thresholds are constrained to the range $[-1, 1]$. The neural network structure is determined to be 3–m–2, which implies that the chromosomal length is $3 \times m + m \times 2 + 2 \times 1$.
(2) The fitness value associated with each combination of weights and thresholds is computed. The discrepancy between the forecasted and actual values is used to ascertain the compensatory impact of the alignment on the exposure machine.
(3) The selection process includes selecting individuals with superior fitness values from the offspring population to become new parents. This is accomplished by calculating the distribution probability using a roulette wheel mechanism.
(4) The study utilized the single-point crossover principle to execute the crossover operation, which enhances the glob-al search capability of the algorithm by exchanging genes among a set of chromosomes to generate new individuals.
(5) Mutation operations alter an individual's genetic locus, creating alternative alleles for substitution, thereby generating a new individual, enhancing the algorithm's global exploration capabilities.
(6) The procedure involves calculations to verify if the latest weights and thresholds meet the fitness value and accuracy requirements of the exposure-machine alignment, and if not, the process is repeated.
(7) The optimum solution is output as the starting weight and threshold of the BP neural network when the required standards are achieved.

3.4.3. *Prediction using optimized BP neural network.* The BP neural network is optimized using GA to determine initial weights and thresholds, and then the neuron parameters are produced and given into the model for predicting the alignment compensation for the exposure machine [13]. The data type and properties, and the specific implementation methods are as follows determine the neural network parameters:

(1) The obtained initial weights and thresholds are assigned to each neuron of the BP neural network.

(2) The Powell–Beale conjugate gradient is used as the activation function and gradient principle of descent. Tansig, the transfer function, defines the input layer to the hidden layer, Pureline, the hidden layer to the output layer, and 1000 is the maximum number of iterations and 0.03 is the learning rate for the appropriate BP neural network con-figuration.
(3) The BP neural network is used to forecast the compensation value, and the correct compensation value is subsequently achieved.

The comprehensive process of algorithm computation is illustrated in Figure 6.

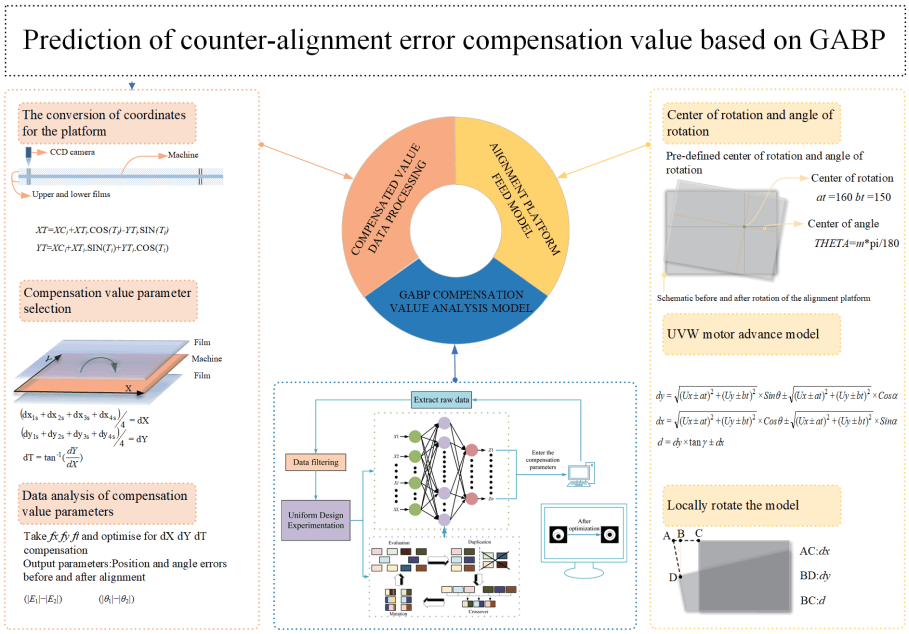

FIGURE 6. Flowchart of experiment.

4. Simulation of compensation values using GABP

In this study, the GA-optimized BP neural network was used to properly anticipate error compensation for the exposure machine. The resulting deviation is utilized as an output, while compensation parameters are employed as inputs. The initial data of the experiment are obtained by aligning the coordinates of the positioning points of the platform to read the experimental data from the upper computer. The data is analyzed to obtain the essential deviation values, the input parameters are determined based on the positional error parameter compensating effect, and computed for the outputs, as shown in Figure 7.

4.1. **Data acquisition and optimization.** The study employed a uniform experimental design to improve the accuracy and stability of the exposure-machine alignment-compensation prediction system. Reliability was achieved by preprocessing the data, increasing the number of spatial points, and using GA-optimized BP

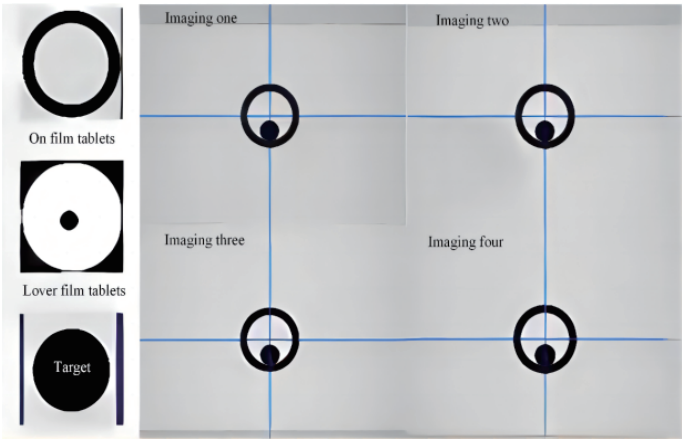

FIGURE 7. Computerized alignment process.

neural networks. Test data was set up to validate the predicted compensation effect, and comparisons were made with traditional BP neural networks to ensure alignment with expected effects.

TABLE 1. Partial data on position error compensation.

Coating mask X direction value (μm)	**Coating mask Y direction value(μm)**	**Rotation angle compensation value of hood (rad)**
31.2	3.8	0.00029
30.3	4.7	0.00029
30.6	3.4	0.00029
30.5	3.3	0.00029
32.3	2.8	0.00029
31.5	1.9	0.00029
32.6	-5.9	0.00029
32.6	-7.9	0.00029
33.4	-9.2	0.00029
33.7	-9.4	0.00029
34.1	-10.2	0.00029
32.6	-12	0.00029
33.9	-12	0.00029
32.2	-12	0.00029
33.3	-10.6	0.00029
34.3	-10.1	0.00029

The alignment platform gap, CCD lens resolution, and compensation value are the three main elements that affect the alignment precision of the exposure machine. The precision of exposure alignment can be increased with an appropriate error-compensation prediction system. The results of the study indicate that the

proposed GABP algorithm can significantly reduce overall performance by improving exposure accuracy, iteration time, and alignment machine alignment time when combined with research on alignment platform error sources and compensation parameters.

TABLE 2. Partial data on position error compensation.

Coating mask X direction value (μm)	**Coating mask Y direction value(μm)**	**Rotation angle compensation value of hood (rad)**	**Output deviation**
1.7	-4.6	-0.00059	1.6385373
0	-1.5	0.00074	0.8727199
2.8	0.9	0.00084	0.6270690
16.6	-8.3	0.00031	-0.043866
24.1	-19.9	0.00027	0.2963287
25.1	-20.6	0.00028	0.8695682

TABLE 3. Hidden layer parameters.

The number of neurons in the hidden layers	**MSE (μm)**	**Validation R**	**Test R**
5	0.032392	0.85512	0.85761
6	0.028974	0.88186	0.89685
7	0.016026	0.92477	0.91491
8	0.054434	0.78079	0.81558
9	0.026439	0.88842	0.91852
10	0.033514	0.87746	0.88475
11	0.0292	0.80075	0.86174
12	0.068954	0.70168	0.53669

The prediction of alignment compensation for the exposure machine uses three parameters, i.e., *fx*, *fy*, and *ft*, as the compensation. To fulfill the accuracy requirements of nonlinear data fitting, a large amount of data was collected to train the prediction system model. The error correction range of *fx* was $[-15, 75]$, *fy* was $[-20, 20]$, and that of *ft* was $[-0.0006, 0.0017]$. In the experiment, a total of 670 sets of position-error compensation parameters were selected for iterative optimization. The experimental results indicated that the number of neurons in the hidden layer was 7. Table 1 provides data for position-error compensation parameters used in experiments, Table 2 presents data from 600 experiments, and Table 3 lists MSE values for different neurons in the hidden layer of the BP neural network.

4.2. **Analysis of results.** The accuracy of the GABP algorithm model was verified by selecting 670 data sets, with 600 used for training and 70 for testing, and iteration was conducted until errors stopped decreasing. The iteration termination conditions

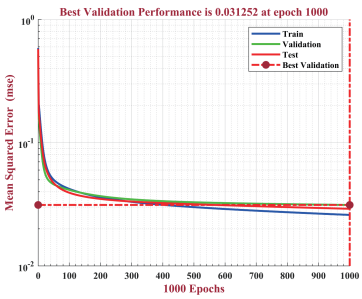

FIGURE 8. MSE of BPNN.

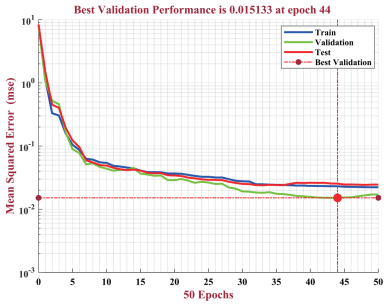

FIGURE 9. MSE of GABP.

were a final accuracy (in terms of error) less than 10^{-3} or a training epoch number greater than 1000.

When GABP is used to predict alignment compensation for the exposure machine, appropriate GA parameters are selected to optimize the weights and thresholds for the BP neural network. The population size Ps in this study was 150, the number of iterations was 50, the crossover rate Pc was set to 0.3, the mutation rate Pm to 0.1, and the solution accuracy was set to 10^{-3}. The acquired results were assessed using a range of metrics, including the R-value, curves of the predicted and actual values, and percentage of the prediction error, after the initial weight threshold of the BP neural network was optimized. The GA-optimized BP neural network outperformed the traditional BP neural network in predicting better compensation values for the alignment compensation system of the exposure machine, resulting in a better alignment effect.

Figure 8 displays the outcomes of using only the BP neural network to improve the position-error correction parameters of the exposure machine in a multi-objective way. The MSE is the average of the sum of squares of the anticipated and original data points, which correspond to the positional error compensation parameter. The accuracy of the prediction model increases with decreasing MSE value. In Figure 8, the MSE value is 0.031252, which is never optimal after 1000 iterations and results in the partial creation of the ideal solution. Furthermore, the optimal MSE value derived from the verification data was higher than the values for the testing and training data. This observation suggests that obtaining an optimal solution for the multi-objective hybrid optimization problem using only a BP neural network is challenging and time-consuming. Conversely, for the multi-objective problem of deter-mining optimal exposure-machine compensation parameters, a hybrid optimization method combining the BP neural network and GA swiftly reached the best MSE value by the 50th iteration, as seen in figure 9. The result, 0.015133, is a significant 72.1% year-on-year drop compared to the prior technique, significantly reducing prediction errors and accelerating the realization of the optimal MSE value.

The R-value test results for the compensation values predicted for the exposure machine using the BP neural network and GABP hybrid optimization method are shown in Figures 10 and 11. A lower deviation indicates that the forecast more closely matches the actual value when the validation R-value is closer to 1. The

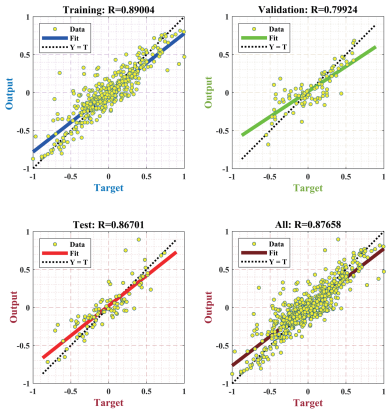

FIGURE 10. R value of BPNN.

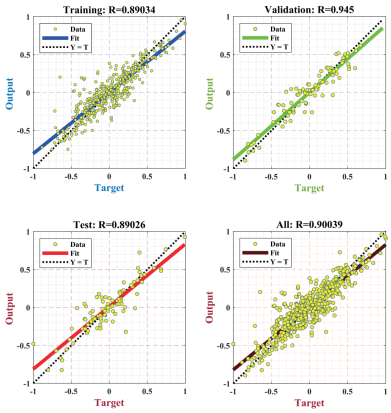

FIGURE 11. R value of GABP.

R-value for the validation data was only 0.79924 when the BP neural network was the only method used to anticipate the compensation value; in contrast, the R-values for the training and test data were 0.89004 and 0.86701, respectively. By con-trast, when the BP neural network optimized by GA was used to predict the compensation value, an outstanding accuracy of 0.945 was achieved in validation, signifying a noteworthy enhancement in the prediction accuracy that corresponded to a remarkable 18.4% year-on-year increase. Evidently, the optimization of the BP neural network significantly increases the prediction accuracy and stability of the model, thereby improving on the countermelody effect of the compensation value.

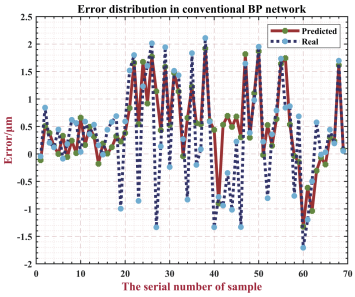

FIGURE 12. Error distribution for BPNN.

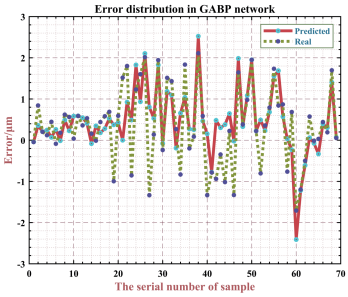

FIGURE 13. Error distribution for GABP.

The error distribution of the optimization results obtained after employing primarily the BP neural network is displayed in Figure 12. The study found significant fluctuations in the 70 predicted compensation parameters values, with an average fitting effect, and a general difference of 3–4 μm in the actual values, based on the difference between actual and predicted values. In contrast, the distribution of the actual errors was more similar to the projected data when the hybrid optimization calculation was used (Figure 13). The fitting impact was better and the first 20 prediction results were more consistent with the actual values. The combination

of BP neural network and GA effectively reduced the number of alignments of the exposure machine during the production process, resulting in a maximum deviation of $3\,\mu m$.

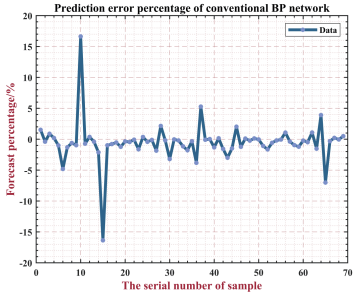

FIGURE 14. Prediction error of BPNN.

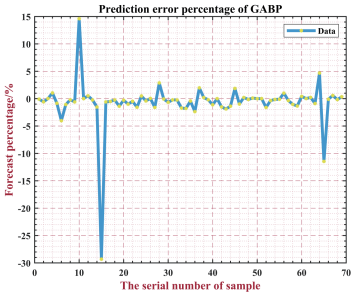

FIGURE 15. Prediction error of GABP.

The proportion of anticipated data mistakes in the actual data errors was mostly kept at 5% when the BP neural network was the sole one employed (figure 14). Figure 15 illustrates that the data was highly inconsistent with a small percentage being steady. However, when the hybrid optimization approach, which included GA, was utilized, the data's stability increased dramatically. The number of errors was reduced to less than 3%, and prediction precision increased by 40%, thereby reducing the time required for the alignment process and improving alignment performance.

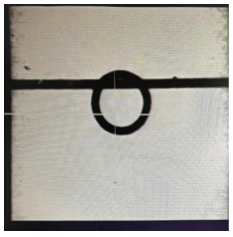

FIGURE 16. Center-to-edge alignment effect.

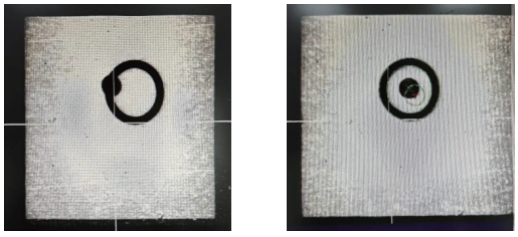

FIGURE 17. Point-to-center alignment effect.

To verify the feasibility of the proposed hybrid method in improving alignment accuracy and efficiency, two experiments on circular center alignment and linear center alignment were performed. Figures 16 and 17 illustrate the impact of the method on alignment, respectively. The alignment accuracy and efficiency have been significantly enhanced, effectively enhancing the alignment accuracy of the exposure process. Thus, the multi-objective hybrid optimization method for the position-error compensation parameters significantly improves the effect of the alignment process of the exposure machine. Although the proposed method uses only neural networks and genetic algorithms combined into a uniform design, it offers innovations in the derivation and use of error compensation parameters. Moreover, from a comparison of the experimental results, it was confirmed that GABP could obtain

error compensation parameters faster and, at the same time, improve the production efficiency. The uniform experimental design provided a wider sample space and controlled the number of experiments. Additionally, the suggested GABP network has been demonstrated as being sufficiently accurate and to be a more efficient prediction approach when compared to the conventional method.

5. Conclusion

In this study, we optimized experimental data using a uniform design of experiments, proposed a prediction method for the alignment compensation systems of exposure machines using a BP neural network optimized by a GA, and analyzed the alignment effect on a flexible-film exposure machine as an example. It was found that using a GA-optimized BP neural network to predict alignment compensation for an exposure machine can effectively reduce the number of iterations and improve alignment accuracy. The suggested approach can forecast the alignment compensation and, based on the data acquired, may predict the next step in real time. This reduces the alignment time greatly, which is realistically useful for real-world engineering applications. The GABP algorithm model does not readily fall into local optimum solutions and can anticipate compensation values with high accuracy, effectiveness, and stability at a fast convergence speed. The prediction results are closer to the ideal alignment compensation effect compared to that provided by the typical BP neural network, and it is extremely unlikely that iterative optimization would be ineffective.

References

[1] K. Ahmadi and A. Carnicer, *Optical visual encryption using focused beams and convolutional neural networks*, Optics and Lasers in Engineering **485** (2022), 3–6.

[2] F. I. Chou, Y. K. Tsai, Y. M. Chen, J. T. Tsai and C. C. Kuo, *Optimizing Parameters of Multi-Layer Convolutional Neural Network by Modeling and Optimization Method*, IEEE Access **7** (2019), 68316–68330.

[3] J. S. Dong, X. Y. Sun and B. Y. Niu, *2021 Comparison of the orthogonal and homogeneous experimental design methods*, Science Technology Vision **22** (2021): 78.

[4] S. E. Ghiasian and K. Lewis, *A recommender system for the additive manufacturing of component inventories using machine learning*, Journal of computing and information science in engineering **22** (2022): 011006.

[5] J. Hao and J. Yan, *Knowledge acquisition of self-organizing systems with deep multiagent rinforcement learning*, Journal of Computing and Information Science in Engineering **22** (2022), 021030–021032.

[6] P. Y. Hao, J. W. Zhu, J. L. Liao, L. L. Zheng and H. Zhang, *Process control and optimization of ingot crystalline silicon growth using neural network and genetic algorithm*, Journal of Synthetic Crystals **51** (2022), 386–389.

[7] H. J. Jin, *Application of advanced BP neural network in image recognition*, in: Proceedings of 2019 18th International Symposium on Distributed Computing and Applications for Business Engineering and Science, IEEE, 2019, pp.17–20.

[8] H. T. Kim, C. S. Song and H. J. Yang, *2-Step algorithm of automatic alignment in wafer dicing process*, Microelectron Reliab **44** (2004),1165–1179.

[9] W. Krattenthaler, K. J. Mayer and M. Zeiller, *Point correlation: Areduced-cost template matching technique*, in: Proceedings of 1994 International Conference on Image Processing, IEEE, 1994, pp. 208–212.

[10] S. Kwon and J. Hwang, *Kinematics,pattern recognition and motion control of mask-panel alignment system*, Control Engineering Practice **19** (2011),883–892.
[11] B. K. Liu, N. V. Bac, X. Y. Zhuang, W. Z. Lu, X. L. Fu and T. Rabczuk, *Al-DeMat: A web-based expert system platform for computationally expensive models in materials design*, Advances in Engineering Software **176** (2023): 103398.
[12] B. K. Liu and W. Z. Lu, *Surrogate models in machine learning for computational stochastic multi-scale modelling in composite materials design*, Journal of Hydromechatronics **5** (2022), 336–365.
[13] B. K. Liu, W. Z. Lu, T. Rabczuk, T. Olofsson and Y. Z. Wang, *Multi-scale modeling in thermal conductivity of Polyurethane incorporated with Phase Change Materials using Physics-Informed Neural Networks*, Renewable Energy **220** (2023): 119565.
[14] S. L. Li, C. Q. Liu, D. Q. Dong and J. W. Qiu, *Application of automatic compensation of color film expose Machine in high fine products*, Optics Optoelectronic Technology **19** (2021), 96–99.
[15] L. K. Malashkhia, D. H. Liu, Y. L. Lu and Y. Wang, *Physics-constrained bayesian neural network for bias and variance reduction*, Journal of Computing and Information Science in Engineering **23** (2023): 011012.
[16] W. J. Qian, J. Li, J. G. Zhu, W. F. Hao and L. Lei, *Distortion correction of a microscopy lens system for deformation measurements based on speckle pattern and grating*, Optics and Lasers in Engineering **124** (2020), 17–26.
[17] N. M. Thoppil, V. Vasu and C. S. P. Rao, *Bayesian optimization LSTM/bi-LSTM network with self-optimized structure and hyperparameters for remaining useful life estimation of lathe spindle unit*, Science Technology and Engineering **22** (2022): 12.
[18] J. T. Tsai, C. C. Chang, W. P. Chen and J. H. Chou, *Data-driven modeling using system integration scaling factors and positioning performance of an exposure machine system*, IEEE Access **5** (2017), 7826–7838.
[19] J. T. Tsai, P. Y. Yang and J. Y. Chou, *Data-driven approach to using uniform experimental design to optimize system compensation parameters for an au-to-alignment machine*, IEEE Access **6** (2018), 40365–40378.
[20] F. Wang and S. Q. Wu, *A flexible circuit board registration method based on template and DCT transform*, Jisuanji Yu Xiandaihua **10** (2021), 59–61.
[21] Y. F. Wang, H. P. Duan and L. J. Zhang *Optimization of radial guide vane multi-stage pump hydraulic performance based on genetic algorithm-back-propagation neural network*, Science Technology and Engineering **21** (2021), 292–297.
[22] Y. Z. Wang, T. L. Han, X. Jiang, Y. H. Yan and J. Hu, *Application of improved genetic algorithm in path planning of step DMD digital mask lithography*, in proceedings of 2020 IEEE International Conference on Artificial Intelligence and Computer Applications, IEEE, 2020, pp. 681–686.

Appendix A. Addendum

GA	Genetic Algorithm
GABP	Genetic Algorithm Optimization of BP Neural Networks
BP	Back Propagation
PCB	Printed Circuit Board
CCD	Charge Coupled Device
MSE	Mean-Square Error

Manuscript received June 4, 2024
revised October 10, 2024

J. Xi
Key Laboratory for Optical Sensing and Testing Technology in Mechanical Industry, Zheng Zhou, China

School of Intelligent Mechatronic Engineering, Zhongyuan University of Technology, Zheng Zhou, China
E-mail address: xjpyq2010@zut.edu.cn

Z. Nie
School of Intelligent Mechatronic Engineering, Zhongyuan University of Technology, Zheng Zhou, China
E-mail address: Zi-Kai.Nie@foxmail.com

L. Deng
School of Intelligent Mechatronic Engineering, Zhongyuan University of Technology, Zheng Zhou, China
E-mail address: 6776@zut.edu.cn

Y. Yue
School of Intelligent Mechatronic Engineering, Zhongyuan University of Technology, Zheng Zhou, China
E-mail address: yyg6970019@126.com

Q. Yang
Center for Modern Educational Technology, Zhongyuan University of Technology, Zheng Zhou, China
E-mail address: yq1317@zut.edu.cn